Syntheses and Crystal Structures of Four Alicyclic Diols which Crystallise in Different Lattices involving Helical Extensions

Stephen C. Hawkins, Roger Bishop,* Donald C. Craig, Ian G. Dance, A. David Rae and Marcia L. Scudder
School of Chemistry, The University of New South Wales, Kensington, New South Wales 2033, Australia

In an exploration of the possibility of modifying the shape and size of the helical canal host structure known to occur in crystals of several bi- and tri-cyclic diols, we report the syntheses and structures of four further diols: 4,8-dimethyl-2-thiatricyclo[3.3.1.1^{3,7}]decane-*syn*-4,*syn*-8-diol **5**; 4,8-dimethyl-2-thiatricyclo[3.3.1.1^{3,7}]decane-*syn*-4,*anti*-8-diol **6**; 2,7-dimethyltricyclo[4.3.1.1^{3,8}]undecane-*syn*-2,*anti*-7-diol **7**; and 2,8-dimethyltricyclo[5.3.1.1^{3,9}]dodecane-*anti*-2,*anti*-8-diol **8**. All four comprise a class of diols with crystal structures involving hydrogen bonded helices, and all but **7** are resolved into conglomerates on crystallisation. Diols **5** and **6** form closely-related helical columns in space group $P4_1$ and $P4_3$ respectively, with only van der Waals attractions between adjacent columns. These structures also involve intramolecular S···H–O hydrogen bonds giving five-membered cycles which persist in solution. Diol **7** crystallises in space group $Pna2_1$ with a three-dimensional hydrogen bonded structure involving recurved spirals with a 4-fold diol repeat. The final diol **8** crystallises in space group $P3_121$ as a further member of the helical tubuland canal structural family, but with void spaces insufficient for inclusion of guest molecules. The structures are discussed with respect to crystal engineering aspects of synthesis.

We have previously shown that diols **1–4** crystallise as conglomerates with a novel helical structure containing tubular void spaces which are capable of trapping guest molecules.[1,2] This helical tubuland[3] lattice is remarkable in that its general structural features remain constant while the molecular structure of the diol building-block is modified. Consequently, these compounds crystallise as a family of helical tubulands with a range of quite different canal sizes, topologies, and inclusion properties.[4]

1

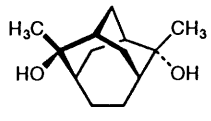

2

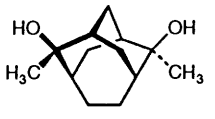

3

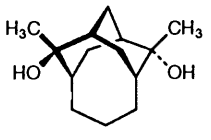

4

These results indicated that it should be possible to design and synthesise other alicyclic diols which would also adopt this host lattice. We have therefore investigated the behaviour of an exploratory series of compounds with the general structure (**I**), in which the variables A, B, C, D, E, F have been systematically varied. Our intention has been to identify the features present in the diol molecular structure which cause formation of this particular lattice type. The aim here is to allow us to predict new examples of these inclusion hosts.

As a result of this study we have found that alicyclic diols of the general structure (**I**) tend to form crystal lattices of two distinct major types. We have recently reported the structures of a set of seven diols, all of which crystallise in layer structures, containing both diol enantiomers and without inclusion properties.[5] In all these lattices four diol molecules each contribute one hydroxy group to produce a cyclic hydrogen-bonded sequence $(-OH)_4$. Involvement of the second hydroxy

I

group of each diol in a neighbouring cyclic arrangement propagates the layer of diol molecules in one plane.

We report here the structures of four diols **5–8** where extended linear hydrogen-bonded sequences lead to helical arrangements of the diol units. These compounds are: 4,8-dimethyl-2-thiatricyclo[3.3.1.1^{3,7}]decane-*syn*-4,*syn*-8-diol **5**; 4,8-dimethyl-2-thiatricyclo[3.3.1.1^{3,7}]decane-*syn*-4,*anti*-8-diol **6**; 2,7-dimethyltricyclo[4.3.1.1^{3,8}]undecane-*syn*-2,*anti*-7-diol **7**; and 2,8-dimethyltricyclo[5.3.1.1^{3,9}]dodecane-*anti*-2,*anti*-8-diol **8**.

In accord with our previous papers in this area[1,5] we designate substituent groups as *syn* or *anti* with respect to the unique largest bridge, or the heteroatom bridge, of the tricyclic system. Diol **7** is the single epimer of **2** and **3**, whereas diol **8** is the double epimer of **4**.

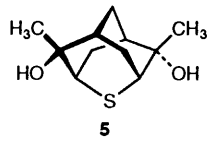

5

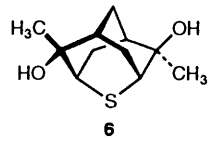

6

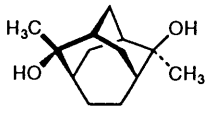

7

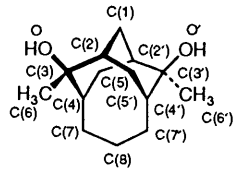

8

Results

Syntheses.—The synthetic routes to the diols **5–8** follow the methodology described previously[5] and are outlined in

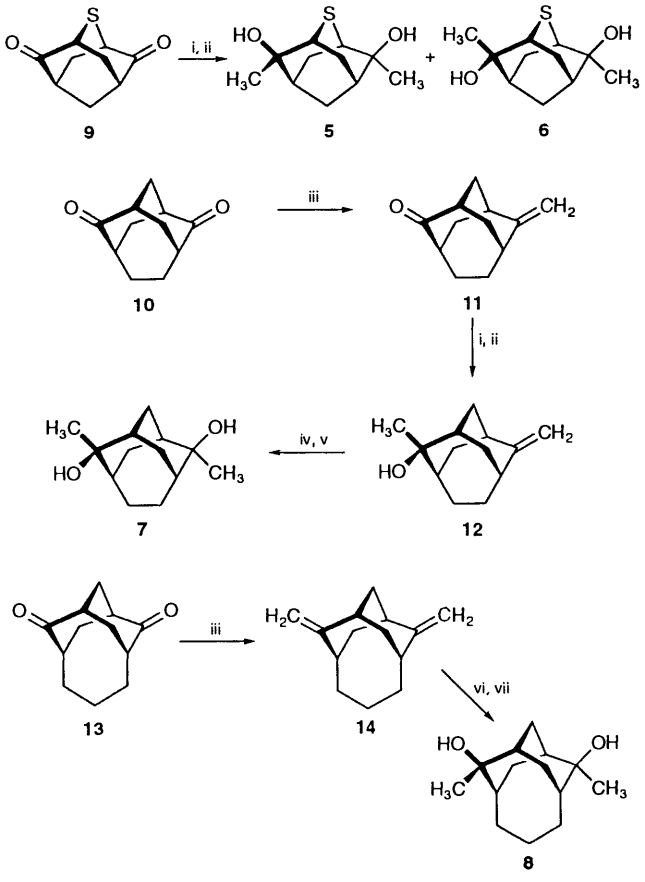

Scheme 1 *Reagents:* i, CH_3MgI; ii, H_3O^+; iii, $Ph_3P{=}CH_2$; iv, $Hg(OAc)_2/H_2O$; v, $NaBH_4/NaOH$; vi, *m*-Cl–C_6H_4–CO_3H; vii, $LiAlH_4$

Scheme 1. Methylation of the thiaadamantane dione **9** took place predominantly from the opposite side to the sulfur atom producing the *syn,syn*-isomer **5** (77%), the *syn,anti*-isomer **6** (15%), and the *anti,anti*-isomer **15** (1%). Diols **5** and **6** were then separated by column chromatography. Diene **14** proved to be almost inert to the mercuric acetate hydration procedure[6] after reaction of the first double bond. (Conversely diol **8** was found to dehydrate abnormally readily, particularly in the presence of traces of acid.) Consequently diol **8** was prepared by the alternative epoxidation–reduction sequence indicated.

The diols **5**–**8** were tested for potential inclusion properties by recrystallisation from each of six standard solvents (benzene, acetonitrile, ethyl acetate, chloroform, acetone, and diethyl ether). Diols **5** and **6** were also tested with ethanol, ethane-1,2-diol, and 1-chloropentane. Following filtration the crystals were dried in a stream of air for 5 min. Paraffin mull IR spectra were then recorded and compared with the original sample. The samples crystallised from ethanol and ethane-1,2-diol were also examined by ^1H NMR spectroscopy. No evidence of inclusion was apparent for compounds **5**–**7**. Diol **8** showed exceptionally weak solvent IR peaks for all of the standard liquids except acetonitrile. These signals were far weaker than previously observed for diol inclusion compounds and they are regarded as being equivocal. Possibly traces of solvent were occluded in occasional crystal faults.

Description of the Structures.—Crystals for X-ray diffraction analysis were recrystallised from acetone (**5** and **6**), ethyl acetate (**7**), and an ethyl acetate–methanol mixture (**8**). The common atom labelling scheme is illustrated on structure **8**, and is the same as that previously used[1] to describe the structures of **1**–**4**. The prime indicates two-fold symmetry (approximate in **5**, **6** and **7**; exact in **8**). Numerical details of the solution and refinement of the structures **5**–**8** are presented in Table 1. Bond lengths and angles for these structures are presented in Tables 2 and 3 respectively. Table 4 contains dimensions associated with the hydrogen bonding.

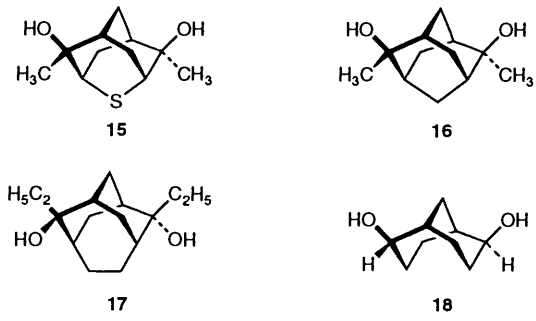

The diols **5** and **6** crystallise in tetragonal space groups with similar unit cell dimensions (Table 1). They both form helical chains where each molecule is linked to the next by a single hydrogen bond. There are four molecules in the repeat unit, related by a 4-fold screw operation (4_1 in space group $P4_1$ for **5**, and 4_3 in $P4_3$ for **6**). In the structure of **5** the second hydroxy hydrogen is bonded intramolecularly to sulfur at a distance of 2.42 Å, and forms angles at sulfur with the bridgehead carbons of only 67.7° and 93.5° (Fig. 1). Similarly the *syn*-hydroxy group of **6** is hydrogen bonded to sulfur at a distance of 2.31 Å and forms angles at sulfur with the bridgehead carbons of 67.3° and 92.3°.

The sulfur containing diols **5**, **6** and **15** are all isomeric. Diol **15** crystallises with an unresolved layer structure in the same way as its carbocyclic analogue, the adamantane derivative **16**.[5] Recrystallisation of **5** and **6** from diethyl ether gave guest-free octahedral crystals with almost identical melting points (153 and 154.5 °C) which are about 35 °C lower than that of **15**. They are also significantly more soluble than **15**. These differences reflect their one-dimensional hydrogen-bonding type compared to the two-dimensional arrangement in **15**.

In **5** and **6**, spontaneous chiral resolution has taken place with both of these diols being obtained as a conglomerate with one molecule per asymmetric unit. It is interesting to note that the cell volume per molecule is almost invariant for the three isomers (263.7 Å^3 in **5**, 264.2 in **6** and 265.7 in **15**), and also for **16** (263.2 Å^3). Clearly the lack of saturation of hydrogen bonding capability in **5** and **6** leads to packing which is no less efficient.

As noted previously the structures of **5** and **6** are essentially the same. The helical chains and their packing arrangement lead to two types of narrow channels surrounding four-fold screw axes in the *c* direction. There is no room for guest inclusion on either axis. Fig. 2 shows the view down the channel formed within the hydrogen bonded helices in **5** and **6**. In contrast, Fig. 3 shows the view down the second channel formed where these helical arrangements abut. The diols around these channels are not linked by hydrogen bonds and only van der Waals interactions are involved. In **5** the sulfur atom of each molecule lies on the inner surface of the hydrogen bonded channel whereas in **6** the sulfur atoms lies on the inner surface of the other channel.

The channels within the helical columns are formed by a

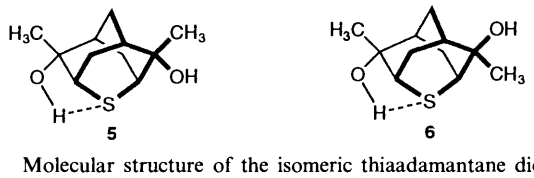

Fig. 1 Molecular structure of the isomeric thiaadamantane diols **5** and **6** showing the intramolecular S···H–O hydrogen bonding arrangement

Table 1 Crystallographic details for **5**, **6**, **7** and **8**

	5	**6**	**7**	**8**
Formula	$C_{11}H_{18}O_2S$	$C_{11}H_{18}O_2S$	$C_{13}H_{22}O_2$	$C_{14}H_{24}O_2$
Formula mass	214.3	214.3	210.3	224.3
Crystal description	{012}{01$\bar{2}$}	(001)(00$\bar{1}$) (012)(0$\bar{1}\bar{2}$) (−1−5 10)(02−3) (102)(10−2)(−100)	{111}{11 − 1}	{100}{101}
Space group	$P4_1$	$P4_3$	$Pna2_1$ (pseudo *Pnan*)	$P3_121$
a/Å	6.5507(2)	6.5793(2)	9.5900(7)	12.3430(4)
b/Å	6.5507(2)	6.5793(2)	10.3411(6)	12.3430(4)
c/Å	24.581(2)	24.417(2)	11.3868(6)	6.8288(3)
V/Å^3	1054.80(8)	1056.92(7)	1129.2(1)	900.99(4)
T/°C	21(1)	21(1)	21(1)	21(1)
Z	4	4	4	3
D_{calc}/g cm^{-3}	1.35	1.35	1.24	1.24
Radiation, λ/Å	Cu-Kα	Cu-Kα	Cu-Kα	Cu-Kα
μ/cm^{-1}	24.5	24.4	6.0	5.9
Crystal dimensions/mm	0.20 × 0.22 × 0.26	0.25 × 0.25 × 0.30	0.20 × 0.20 × 0.20	0.20 × 0.18 × 0.30
Scan mode	$\theta/2\theta$	$\theta/2\theta$	$\theta/2\theta$	$\theta/2\theta$
$2\theta_{max}$/°	140	140	120	140
No. of intensity measurements	1208	1249	1041	3410
Criterion for obsd. reflection	$I/\sigma(I) > 3$	$I/\sigma(I) > 3$	$I/\sigma(I) > 3$	$I/\sigma(I) > 3$
No. of indep. obsd. reflections	999	969	721	613
No. of reflections (m), variables (n) in final refinement	999, 136	969, 132	721, 202	613, 82
$R = \Sigma^m\|\Delta F\|\Sigma^m\|F_0\|$	0.023	0.030	0.046	0.030
$R_w = [\Sigma^m w\|\Delta F\|^2/\Sigma^m w\|F_0\|^2]^{\frac{1}{2}}$	0.029	0.039	0.055	0.039
$s = [\Sigma^m w\|\Delta F\|^2/(m - n)]^{\frac{1}{2}}$	1.23	1.51	1.91	2.43
Crystal decay	1 to 0.95	none	none	
Max., min. transmission coefficient	0.69, 0.59	0.70, 0.56	0.92, 0.90	0.93, 0.85
Extinction coefficient	—	—	—	2.09 × 10^{-3}
Largest peak in final diff. map/e Å^{-3}	0.20	0.19	0.22	0.15

Table 2 Bond lengths (Å) for **5**, **6**, **7** (the major component) and **8**

	5	**6**	**7**	**8**
C(1)–C(2)	1.538(3)	1.533(3)	1.565(8)	1.531(2)
C(1)–C(2′)	1.532(3)	1.533(4)	1.555(9)	
C(2)–C(3)	1.533(3)	1.542(4)	1.550(9)	1.545(2)
C(2′)–C(3′)	1.546(3)	1.548(4)	1.538(9)	
C(3)–C(4)	1.541(3)	1.542(3)	1.540(9)	1.548(2)
C(3′)–C(4′)	1.549(3)	1.534(4)	1.541(9)	
C(4)–C(5)	1.535(3)	1.530(3)	1.529(11)	1.548(3)
C(4′)–C(5′)	1.527(3)	1.529(4)	1.519(11)	
C(5)–C(2′)	1.536(3)	1.540(4)	1.533(10)	1.539(3)
C(5′)–C(2)	1.538(3)	1.542(4)	1.532(10)	
C(3)–O	1.432(3)	1.447(3)	1.456(4)	1.455(2)
C(3′)–O′	1.433(3)	1.440(3)	1.451(4)	
C(3)–C(6)	1.528(4)	1.522(4)	1.525(6)	1.525(2)
C(3′)–C(6′)	1.523(4)	1.523(4)	1.527(5)	
S–C(4)	1.825(2)	1.836(3)		
S–C(4′)	1.828(2)	1.821(3)		
C(4)–C(7)			1.494(8)	1.554(3)
C(4′)–C(7′)			1.493(7)	
C(7)–C(8)				1.415(5)
C(7′)–C(8)				1.616(5)
O–HO	0.88(2)	0.89(5)		0.87(3)
O′–HO′	0.80(2)	1.03(5)		

repeating unit of four diol molecules and the absence of any significant free volume within the helices of **5** and **6** is due to there being only four molecules per turn with a pitch angle of about 24.5°. This is also observed in the ellipsoidal clathrate structure of diol **2** with benzene[7,8] where there is a pitch angle of 18.9°. On the other hand the helical tubuland lattices of diols **1**–**4** have six molecules per turn with a pitch angle of about 14°. This smaller angle and higher repeat number produces the open canals of this lattice type. In the helical tubuland structure, where the channel is a result of a six-diol repeat unit,[2] the cross-sectional diameter of the channel can be as high as 8 Å.

Diol **7** crystallised, free of solvent and still racemic, as blocks from ethyl acetate in the orthorhombic space group $Pna2_1$. The structure of **7** contains molecules with each O–H taking part in two hydrogen bonds, one as a donor and one as an acceptor. This was also found in all the layer structures where the sequence of hydrogen bonded diol molecules could be described as being a–b–c–d around any one cycle. Compound **17** is one example of the diols which hydrogen bond employing this motif. In this particular case the cycle $(-OH)_4$ is twisted and has a figure of eight shape in flat projection.[5]

This projection shape is also encountered in the structure of **7** where the hydrogen bonding forms a continuous spine in the *a* direction of the unit cell. Rather than the fourth hydroxy group completing a cycle as in the structure of **17**, it is orientated in the opposite direction creating an infinite four-fold repeat of diol molecules in the sequence –a–b–c–d–a– *etc.* (see Fig. 4). More accurately this spine could be described as a recurved spiral, since in projection it has a figure of eight shape. Only one diol hydroxy group can belong to a given spiral. Therefore the second is subtended to form part of a second spiral and the hydrogen bonded lattice is thus extended into three dimensions. Adjacent spirals are of the opposite handedness producing a lattice with overall achirality.

The structure of diol **18** also has hydrogen bonds in infinite chains comprising a recurved spiral with a figure of eight projection. However here the repeat unit is eight diol molecules.[9] In both **7** and **18** pairs of diols of the same chirality alternate with pairs of the opposite chirality along the spine.

Diol **8** was crystallised from ethyl acetate–methanol as squat needles. X-Ray analysis showed these to be isomorphous with those of diols **1**–**4** in space group $P3_121$. It thus provides a further example of the helical tubuland structure. This structure type contains spiral spines of hydrogen bonds with a 3-fold repeat unit. The propano bridge of the diol C(8) atom was disordered as required by space group symmetry. Refinement

Table 3 Interbond angles (°) for **5**, **6**, **7** (the major component) and **8**

	5	6	7	8
C(2)–C(1)–C(2′)	109.8(2)	109.6(2)	106.7(5)	108.2(2)
C(1)–C(2)–C(3)	110.4(2)	110.7(2)	111.9(5)	110.0(1)
C(1)–C(2′)–C(3′)	111.0(2)	110.0(2)	111.7(5)	
C(1)–C(2)–C(5′)	108.0(2)	108.5(2)	108.9(7)	108.1(1)
C(1)–C(2′)–C(5)	108.2(2)	108.5(2)	107.5(8)	
C(3)–C(2)–C(5′)	111.7(2)	111.4(2)	113.0(7)	117.7(2)
C(3′)–C(2′)–C(5)	111.2(2)	112.4(2)	113.6(6)	
C(2)–C(3)–C(4)	109.7(2)	109.4(2)	111.9(5)	113.1(1)
C(2′)–C(3′)–C(4′)	109.3(2)	109.2(2)	113.0(5)	
C(2)–C(3)–O	106.3(2)	109.8(2)	108.8(5)	106.8(1)
C(2′)–C(3′)–O′	110.1(2)	109.5(2)	102.9(6)	
C(4)–C(3)–O	110.9(2)	109.2(2)	110.6(6)	103.2(1)
C(4′)–C(3′)–O′	109.4(2)	103.8(2)	107.1(5)	
C(3)–C(4)–C(5)	111.2(2)	112.5(2)	112.8(6)	112.3(2)
C(3′)–C(4′)–C(5′)	112.0(2)	111.5(2)	113.5(6)	
C(4)–C(5)–C(2′)	111.3(2)	110.8(2)	114.7(3)	118.6(1)
C(4′)–C(5′)–C(2)	111.7(2)	111.0(2)	114.2(3)	
C(4)–C(3)–C(6)	110.2(2)	112.0(2)	109.0(6)	114.3(2)
C(4′)–C(3′)–C(6′)	111.3(2)	113.5(2)	113.8(6)	
C(2)–C(3)–C(6)	112.9(2)	112.2(2)	108.5(6)	112.2(1)
C(2′)–C(3′)–C(6′)	112.5(2)	113.0(2)	113.8(6)	
O–C(3)–C(6)	106.7(2)	104.1(2)	108.0(5)	106.3(2)
O′–C(3′)–C(6′)	104.0(2)	107.5(2)	105.2(5)	
C(4)–S–C(4′)	95.6(1)	95.6(1)		
C(3)–C(4)–S	110.4(2)	109.5(2)		
C(3′)–C(4′)–S	108.7(2)	110.1(2)		
C(5)–C(4)–S	109.6(2)	108.9(2)		
C(5′)–C(4′)–S	110.0(2)	110.2(2)		
C(3)–C(4)–C(7)			113.6(6)	116.7(2)
C(3′)–C(4′)–C(7′)			114.2(5)	
C(5)–C(4)–C(7)			111.5(8)	115.0(2)
C(5′)–C(4′)–C(7′)			110.1(7)	
C(4)–C(7)–C(7′)			120.4(5)	
C(4′)–C(7′)–C(7)			120.0(5)	
C(4)–C(7)–C(8)				120.6(2)
C(7)–C(8)–C(7′)				119.0(3)
C(3)–O–HO	114(2)	100(3)		109(2)
C(3′)–O′–HO′	107(2)	105(3)		

Table 4 Dimensions (Å and °) associated with hydrogen bonding in **5**–**8**

5			
O···O′[a]	2.856	S···O′	2.964
HO···O′[a]	2.01	S···HO′	2.42
O–HO···O′[a]	164	S···HO′–O′	126
C(3)–O···O′[a]	104.4	C(4)–S···HO′	93.5
O···O′[a]–C(3′)[a]	109.8	C(4′)–S···HO′	67.7
a 1 − *y*, *x*, ¼ + *z*			
6			
O′···O[a]	2.840	S···O	2.983
HO′···O[a]	1.83	S···HO	2.31
O′–HO′···O[a]	166	S···HO–O	132
C(3′)–O′···O[a]	109.1	C(4)–S···HO	67.3
O′···O[a]–C(3)[a]	106.0	C(4′)–S···HO	92.3
a 1 − *y*, *x*, −¼ + *z*			
7			
O···O′[a]	2.974	O···O′[b]	3.085
HO···O′[a]	2.04	HO···O′[b]	2.15
O–HO···O′[a]	169	O···HO′[a]–O′[a]	168
C(3)–O···O′[a]	140.7	C(3)–O···O′[b]	97.9
O···O′[a]–C(3′)[a]	117.0	O···O′[b]–C(3′)[b]	110.3
O′[a]···O···O′[b]	113.2	O···O′[a]···O[c]	120.8
a −*x*, 1 − *y*, ½ + *z*			
b ½ − *x*, ½ + *y*, ½ + *z*			
c −½ + *x*, 1½ − *y*, *z*			
8			
O···O[a]	2.834		
HO···O[a]	1.97		
O–HO···O[a]	171		
C(3)–O···O[a]	108.8		
O···O[a]–C(3)[a]	129.8		
a −*y*, 1 + *x* − *y*, ⅓ + *z*			

gave unequal C(7)–C(8) and C(7′)–C(8) lengths, one being too short for a normal C–C and one being too long. This implies some uncertainty in the position of C(8) which is reflected in the higher standard deviation associated with it. The same phenomenon has been observed in the refinement of the structure of its double epimer **4** with the same helical tubuland lattice.[1,10]

In the case of **8**, the canal void space is even more severely restricted than for the earlier[1,2] homoadamantane analogue **3**. By virtue of their size and their different positions along *c*, the propano bridges interleave slightly at the centre of the canal and there is no longer any free space at the centre of the canal. However three small lateral areas remain giving a total unobstructed cross-sectional area of *ca.* 2.7 Å^2. Additional free space exists in the form of grooves which spiral between the propano bridges along *c*, but, like **3**, these volumes are insufficient for inclusion of guest molecules. Only one orientation of the disordered propano bridges is shown in Fig. 5.

The density of the sample of **8** prepared for crystallography was measured by flotation as 1.23 g cm^{-3}, agreeing very closely with that computed for the diol lattice alone (1.24 g cm^{-3}), and

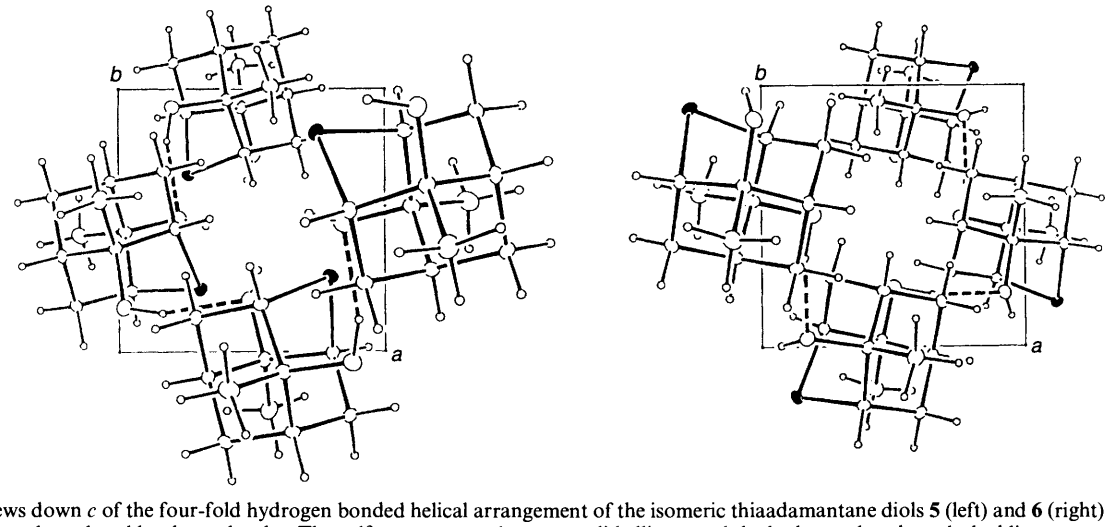

Fig. 2 Views down *c* of the four-fold hydrogen bonded helical arrangement of the isomeric thiaadamantane diols **5** (left) and **6** (right) showing the narrow channels enclosed by the molecules. The sulfur atoms are shown as solid ellipses and the hydrogen bonds as dashed lines.

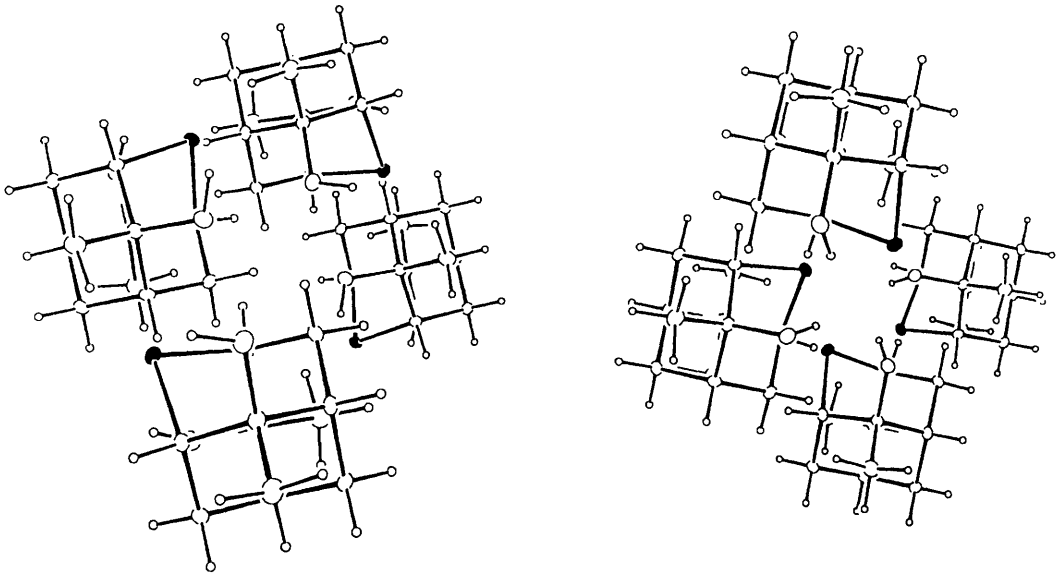

Fig. 3 Views down the second four-fold screw axes of the structures of **5** (left) and **6** (right) showing how four adjacent hydrogen bonded helical columns abut. Only van der Waals forces are present between the diols forming these second types of channel.

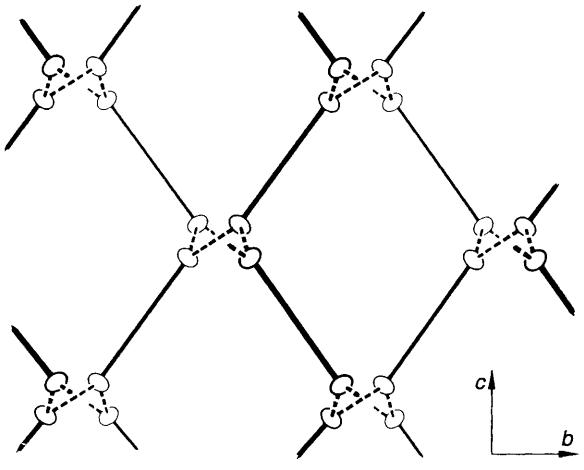

Fig. 4 Schematic hydrogen bonding network of crystalline diol **7** viewed down *a*. Diol molecules are reduced to solid spacer rods and hydrogen bonds are shown as dashed lines in this representation. The recurved spiral arrangement of hydrogen bonds is formed from a four-diol repeat and has a figure of eight shape in projection.

confirming that inclusion did not take place within this diol. The efficient self-filling of the canals (and consequent effective van der Waals attractions) is reflected in the poor solubility of **8** compared with **1**–**4**. This made it impossible to record a ^{13}C NMR spectrum for this compound. Similarly both **3** and **8** have particularly high m.p. values (245–247 and 249–250 °C respectively) compared with the other helical tubuland diols.[1,2]

Discussion

Sulfide–Hydroxy Group Hydrogen Bonding in Crystalline **5** *and* **6**.—A novel feature of the crystal structures of diols **5** and **6** is the presence of intramolecular five-membered S···H–O hydrogen bonds with S···H lengths of 2.42 and 2.31 Å respectively. Although this phenomenon is geometrically impossible for the third thiaadamantane isomer **15**, it is noteworthy that the crystal structure of that diol contained only hydroxy hydrogen bonds.[5] As with **5** and **6**, no intermolecular S···H–O hydrogen bonds are present in the solid state.

We have identified six literature examples of crystal structures containing intramolecular five-membered S···H–O hydrogen bonds (with S···H distance under 2.60 Å in length) between sulfide and hydroxy groups. These are (with S···H distances in Å): bis(1,3-dithian-2-yl)methanol (2.51);[11] 1,1,1-trifluoro-5-phenyl-4-thiapentane-2,2-diol (2.33);[12] 2-hydroxy-4-methyl-3-phenylthiolatomorpholine (2.54);[13,14] (*S*)-4,5-*O*-benzylidene-D-arabinose diethyl dithioacetal (2.26);[15] a derivative of 2-thiatricyclo[4.3.3.0^{1,5}]dodec-4-en-11-one (2.22);[16] and a penicillanic acid derivative (2.56).[17] Although relatively few cases are documented, these examples encompass a diverse range of chemical structures and it is clear that the arrangement encountered in these, and in diols **5** and **6**, is most favourable for molecules where the sulfur atom and hydroxy group are correctly positioned.

^1H *NMR Spectra of* **5**, **6** *and* **15**.—An unusual feature of the ^1H NMR spectra ($CDCl_3$ solution) of the thiaadamantane diols **5** and **6**, relative to the third isomer **15**, requires comment here. The *anti,anti*-diol **15** shows a six proton singlet at 1.63 δ(CH_3 groups) and a two proton singlet at 1.45 δ(OH groups).

In marked contrast, these groups in the *syn,syn*-isomer **5** appear as a six proton doublet (J = 1.26 Hz) at 1.40 δ and a two proton quartet (J = 1.26 Hz) at 3.74 δ. Exchange with deuterium oxide removes the OH signal and causes the doublet to collapse to a six proton singlet.

The unsymmetrical diol **6** shows the *syn*-CH_3 as a singlet at 1.64 δ, the *anti*-CH_3 as a doublet (J = 1.26 Hz) at 1.40 δ, the *anti*-OH as a singlet at 1.52 δ, and the *syn*-OH as a quartet (J = 1.26 Hz) at 3.99 δ. Deuterium exchange removes both OH signals and causes the doublet to collapse to a three proton singlet.

In chloroform solution proton exchange normally prevents observation of the three bond coupling H–O–C–H between a hydroxy hydrogen and its corresponding primary or secondary alcohol hydrogen(s). Such couplings are usually observed in better hydrogen bonding solvents such as dimethylsulfoxide.[18] Here four bond coupling is observed in chloroform solution when the hydroxy group is *syn*, but not when it is *anti*.

The conclusion drawn must be that the *syn*-hydroxy groups in **5** and **6** are strongly hydrogen bonded and this is supported by their high chemical shift values relative to the *anti*-hydroxy groups in **6** and **15**. Such hydrogen bonding presumably involves the sulfur atom. This could occur *via* an aggregate in solution, but the simplest explanation is that the intramolecular

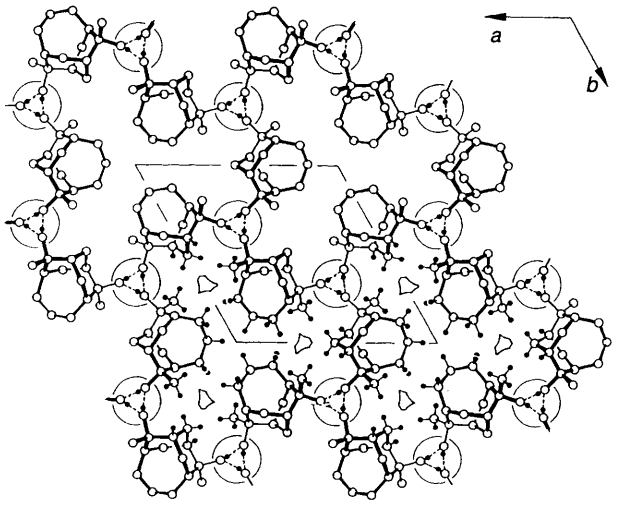

Fig. 5 Projection view in the *ab* plane of the tricyclic diol network in crystalline **8**. Selected hydrogen atoms are shown as filled circles with their van der Waals radii to delineate the small unobstructed areas of the canals. Void spaces within this helical tubuland lattice are insufficient for guest inclusion.

five-membered hydrogen bonding arrangement observed in the solid state is persisting in solution. If so, then the *syn,syn*-isomer **5** has two identical intramolecular S···H–O hydrogen bonds in solution now that the intermolecular O···H–O hydrogen bonding has been lost. Those compounds whose crystal structures[11–17] were discussed above do not appear to exhibit such coupling in the cases where their ^{1}H NMR spectra were also reported. Long range coupling is well known to be highly angle dependent, so presumably the angular geometry in **5** and **6** is such that it is ideal for this phenomenon.

Crystal Lattice Types of Diols **5–8**.—All four diols reported here have lattices involving hydrogen bonded helices, as opposed to the seven compounds reported earlier which had hydrogen bonded cycles leading to layer structures.[5] The helical compounds thus represent a second major class of diol crystal structures of which the helical tubuland lattice may be regarded as a sub-group. Once again, however, this lattice arrangement may be constructed in several distinct ways.

In an earlier paper we attempted to define a set of molecular determinants (membership rules) which could be used to predict probable new members of the helical tubuland lattice,[4,19] and it is noteworthy that these suggestions hold up well in these present cases.

One reason for the failure of **5** and **6** to adopt the helical tubuland lattice is the rigidity of the thiaadamantane skeleton. A degree of twisting between the two ends of the skeleton has been proposed previously to be the reason why the adamantane diol **16** forms a layer structure while its homologues **1–4** form the helical tubuland lattice.[4,19] As discussed earlier, the structures of diols **5** and **6** are essentially the same with different orientation of the diol molecules. In terms of hydrogen bonding their lattices are essentially unidirectional with no inter-column hydrogen bonding being present. Therefore the lattices of **5** and **6** are distinct in that, unlike **7** and **8**, they lack hydrogen bonded spines. Channels are produced in both these structures but they are far too small to afford inclusion properties. The second hydroxy group of **5** or **6** which might have fulfilled the role of intercolumn hydrogen bonding is instead intercepted by the sulfur atom resulting in the intramolecular five-membered cycles discussed above. Clearly the presence of a heteroatom in the ring system in a site where it can compete with the hydroxy groups for hydrogen bonding is deleterious in attempts to use crystal engineering[20] in the construction of new helical tubuland hosts. An even more dramatic example of this property has recently been published.[21]

Whereas diols **2** and **3** have the helical tubuland lattice arrangement, their single epimer **7** does not. This is expected on the consideration that average C_2 symmetry is necessary for a diol to give the helical tubuland lattice.[4,19] The structure actually obtained is a three-dimensional hydrogen bonded lattice, but no diol resolution takes place and the helical spines leave no void spaces for inclusion within the lattice. This structure has close similarities to that of diol **18**[9] as noted earlier. In structural terms **5–7** represent near misses to our target of synthesising more examples of the helical tubulate diols.

Diol **8**, the double epimer of **4**, is the only diol of this series which obeys all six of the molecular determinants[4,19] and it does indeed adopt the helical tubuland arrangement. This diol is the fifth member of these compounds to be discovered. As discussed above, however, this particular structure contains insufficient free volume for inclusion of guest molecules because of the bulky propano bridges occupying most of the canal volume. Very recent work extending the ideas introduced by the molecular determinant approach, and further developed here, has led to the discovery of another two examples of the helical tubuland family. These new compounds are excellent inclusion hosts.[22,23]

Experimental

^{13}C NMR spectra (25.1 MHz) were recorded with a JEOL FX-100 spectrometer, and the substitution of carbon atoms was determined by off-resonance decoupling. ^{1}H NMR spectra were recorded using a Bruker CXP-300 instrument (300 MHz). All spectra are reported as chemical shifts relative to $SiMe_4$. *J*-Values are given in Hz. M.p.s were obtained with a Kofler instrument and are uncorrected. Routine mass spectra (electron impact) were determined with an AEI MS12 spectrometer, the exact mass (chemical ionisation) of **8** with an AEI MS9 spectrometer, and the exact mass (chemical ionisation) of **14** with a Bruker CMS47 FTICR instrument.

4,8-*Dimethyl*-2-*thiatricyclo*[3.3.1.1^{3,7}]*decane*-syn-4,syn-8-*diol* **5**.—A solution of 2-thiatricyclo[3.3.1.1^{3,7}]decane-4,8-dione **9**[24] (0.63 g, 3.43 mmol) in anhyd. tetrahydrofuran (THF) (30 cm^3) was added dropwise to a cold (0–5 °C) stirred solution of methylmagnesium iodide (11 mmol) in dry ether (30 cm^3). The mixture was stirred at room temp. overnight, refluxed for 45 min, and then the cooled reaction worked up by addition of damp ether and separation of the organic layer. After further extraction using ether, the combined extracts were dried ($MgSO_4$), filtered, and solvent evaporated to give a mixture of diol isomers as a white powder (0.69 g, 93%). Column chromatography on silica (chloroform) gave first the *syn,syn*-diol **5** (0.57 g, 77%), m.p. 153 °C (from ether) (Found: C, 61.65; H, 8.6; S, 14.9. $C_{11}H_{18}O_2S$ requires C, 61.6; H, 8.5; S, 15.0%); ν_{max}(paraffin mull)/cm^{-1} 3420m, 3380m, 1140s and 930m; δ_H($CDCl_3$) 1.40 (6 H, d, *J* 1.26, collapses to s on D_2O exch. of OH), 1.77 (2 H, m), 1.93 (2 H, m), 2.09 (2 H, m), 2.54 (2 H, m), 2.65 (2 H, m) and 3.74 (2 H, q, *J* 1.26, exch. D_2O); δ_C($CDCl_3$) 24.9 (q), 31.3 (t), 31.6 (t), 37.3 (d), 44.8 (d) and 68.7 (s); *m/z* 216 (3%), 215 (8), 214 (M^+, 66), 199 (3), 196 (7), 181 (4), 178 (2), 171 (36), 153 (89), 119 (39), 111 (22), 83 (38), 71 (21) and 43 (100).

4,8-*Dimethyl*-2-*thiatricyclo*[3.3.1.1^{3,7}]*decane*-syn-4,anti-8-*diol* **6**.—Further elution of the above column gave next the *syn,anti*-diol **6** (0.11 g, 15%), and finally the *anti,anti*-diol[5] **15** (0.01 g, 1%). Diol **6**, m.p. 154.5 °C (from ether) (Found: C, 61.45; H, 8.6; S, 14.7. $C_{11}H_{18}O_2S$ requires C, 61.6; H, 8.5; S, 15.0%); ν_{max}/cm^{-1} 3380s, 1130m, 1110m and 910m; δ_H($CDCl_3$) 1.40

(3 H, d, J 1.26, collapses to s on D_2O exch. of OH), 1.52 (1 H, s, exch. D_2O), 1.64 (3 H, s), 1.68–1.78 (2 H, m), 2.25–2.42 (6 H, m), 2.48–2.57 (2 H, m) and 3.99 (1 H, q, J 1.26, exch. D_2O); $\delta_C(CDCl_3)$ 24.7 (q), 27.8 (q), 29.1 (t), 30.1 (t), 34.1 (t), 37.2 (d), 37.7 (d), 41.3 (d), 45.7 (d), 68.6 (s) and 71.8 (s); m/z 216 (3%), 215 (8), 214 (M^+, 57), 199 (4), 196 (8), 181 (4), 178 (2), 171 (29), 153 (70), 119 (42), 83 (28), 71 (24) and 43 (100).

7-*Methylenetricyclo*[4.3.1.1^{3,8}]*undecan-2-one* **11**.—A solution of tricyclo[4.3.1.1^{3,8}]undecane-2,7-dione[1,25] **10** (0.35 g, 2 mmol) in dry dimethylsulfoxide (DMSO) (5 cm^3) was added to a stirred solution of methylenetriphenylphosphorane (2.2 mmol) in dry DMSO (15 cm^3) under dry nitrogen as in the Corey method[26] for the Wittig reaction. After heating for 2 h at 75 °C, the cooled mixture was worked up in the usual manner with water and ether. The crude product was sublimed under reduced pressure to obtain slightly impure enone **11** contaminated with trace amounts of the diene[1] and the starting material. A second sublimation gave pure product (0.16 g, 47%), m.p. 131–133 °C (Found: C, 81.7; H, 9.2. $C_{12}H_{16}O$ requires C, 81.8; H, 9.15%); ν_{max}(paraffin mull)/cm^{-1} 3070w, 1705s, 1645w, 1010w, 905m and 895w; $\delta_C(CDCl_3)$ 27.3 (t), 32.3 (t), 33.6 (t), 36.7 (d), 37.0 (t), 38.1 (t), 39.4 (d), 44.9 (d), 47.8 (d), 108.1 (t), 155.0 (s) and 217.5 (s); m/z 176 (M^+, 100%), 161 (4), 158 (7), 143 (28), 130 (21), 129 (24), 119 (15), 117 (14), 105 (31), 91 (60) and 79 (42).

2-*Methyl*-7-*methylenetricyclo*[4.3.1.1^{3,8}]*undecan*-syn-2-*ol* **12**.—A solution of enone **11** (0.18 g, 1.0 mmol) in dry ether (10 cm^3) was added to a stirred solution of methylmagnesium iodide (4 mmol) in ether (15 cm^3) and heated under reflux for 30 min. The reaction was worked up as described for **5**, and the crude solid product purified by column chromatography on alumina (pentane) to yield the enol **12** (84 mg, 44%), m.p. 74–75 °C (from petroleum); ν_{max}(paraffin mull)/cm^{-1} 3390s, 3070w, 1640m, 1110s, 1020w, 930m and 885s; m/z 192 (M^+, 34%), 191 (9), 177 (100), 174 (40) and 159 (18).

2,7-*Dimethyltricyclo*[4.3.1.1^{3,8}]*undecane*-syn-2,anti-7-*diol* **7**.—A solution of enol **12** (0.08 g, 0.42 mmol) in THF (1.5 cm^3, freshly distilled from lithium aluminium hydride) was added to a stirred mixture of mercury(II) acetate (0.14 g, 0.44 mmol), water (2.5 cm^3) and purified THF (2.5 cm^3). After 1.2 h aq. sodium hydroxide (3 mol dm^{-3}; 1 cm^3) was added, followed rapidly by a further 1 cm^3 (also 0.5 mol dm^{-3} in $NaBH_4$). The reaction was stirred for 10 min, then extracted first with petrol and then with ether. After washing (H_2O), the combined extracts were dried ($MgSO_4$), filtered and solvent evaporated to give the diol **7** (65 mg, 74%), m.p. 173–174 °C (from chloroform) (Found: C, 74.1; H, 10.7. $C_{13}H_{22}O_2$ requires C, 74.2; H, 10.5%); ν_{max}(paraffin mull)/cm^{-1} 3440s, 1210w, 1120s, 1110s, 1095s, 1075s, 1030m, 935s, 910m and 890m; $\delta_H[(CD_3)_2SO]$ 1.11 (3 H, s), 1.24 (3 H, s), 1.20–1.55 (6 H, m), 1.57–1.63 (3 H, m), 1.65–1.80 (2 H, m), 1.81–1.86 (1 H, m), 2.00–2.15 (2 H, m), 3.86 (1 H, s, exch. D_2O) and 3.96 (1 H, s, exch. D_2O); $\delta_C[(CD_3)_2SO]$ 27.1 (q), 27.6 (q), 28.1 (t), 29.5 (t), 30.5 (t), 30.5 (d), 32.8 (t), 39.3 (d), 43.1 (d), 43.4 (d), 73.0 (s) and 73.4 (s), plus one peak (t) unresolved; m/z 195 ($M^+ - 15$, 45%), 192 (7), 177 (12), 174 (8), 159 (7), 149 (14), 145 (6), 107 (15), 105 (15), 95 (14), 93 (24), 91 (14), 81 (17), 79 (15), 71 (18), 67 (15), 55 (13), 45 (13), 43 (100) and 41 (22).

2,8-*Dimethylenetricyclo*[5.3.1.1^{3,9}]*dodecane* **14**.—A solution of tricyclo[5.3.1.1^{3,9}]dodecane-2,8-dione[1] **13** (1.5 g, 7.80 mmol) was added as a powder to a stirred solution of methylenetriphenylphosphorane (13.3 mmol) in dry DMSO (30 cm^3) following the procedure described for **11**. Column chromatography of the crude product on alumina (pentane) gave the diene **14** (0.54 g, 37%), m.p. 95–100 °C. This material undergoes rapid polymerisation on standing and in solution [Found (CI): $(M + H)^+$, 189.1646; $C_{14}H_{21}$ requires M, 189.1638]; ν_{max}(film)/cm^{-1} 3070w, 2920s, 1635m, 1455m, 1020w, 890s and 680w; $\delta_H(CDCl_3)$ 1.40–1.54 (4 H, m), 1.62 (4 H, t), 1.71 (2 H, m), 1.9–2.1 (2 H, m), 2.51 (2 H, m), 2.79 (2 H, m), 4.70 (2 H, d) and 4.88 (2 H, d); $\delta_C(CDCl_3)$ 21.6 (t), 35.4 (d), 35.4 (t), 36.3 (t), 36.6 (d), 38.7 (t), 110.6 (t) and 155.0 (s); m/z 188 (M^+, 27%), 173 (19), 159 (12), 147 (29), 145 (23), 131 (41), 119 (22), 117 (25), 105 (73), 94 (88), 93 (63), 92 (37), 91 (100), 81 (23), 79 (38) and 77 (23). Further elution of the column gave 8-methylenetricyclo-[5.3.1.1^{3,9}]dodecan-2-one (0.64 g, 43%).[5]

2,8-*Dimethyltricyclo*[5.3.1.1^{3,9}]*dodecane*-anti-2,anti-8-*diol* **8**.—A solution of *m*-chloroperbenzoic acid (0.31 g of 85% purity) in dichloromethane (3 cm^3) was added dropwise to a vigorously stirred mixture of diene **14** (0.14 g, 0.72 mmol), dichloromethane (3 cm^3) and aq. sodium hydrogen carbonate (0.5 mol dm^{-3}; 2 cm^3). After 1 h, aq. sodium sulfide was added to destroy remaining peracid, and the organic layer separated. The mixture was extracted with further dichloromethane, then the combined extracts washed (H_2O) and dried ($MgSO_4$). Solvent was then evaporated from the filtrate to give the bis(epoxide) as a gum. This crude material was dissolved in dry ether (10 cm^3) and stirred with excess lithium aluminium hydride for 12 h at room temp. Excess reagent was destroyed by addition of damp ether and the lithium salts were just dissolved with dil. hydrochloric acid. Most of the product remained as a solid at the interface of the organic and aq. phases and was separated by filtration. Further material was obtained by thorough extraction with ether, followed by washing of the organic extracts (aq. $NaHCO_3$), drying ($MgSO_4$), and evaporation of the filtrate. The crude product was crystallised from methanol to yield the diol **8** (70 mg, 44%), m.p. 249–250 °C [Found (CI, pyridine and hydrogen): (M + H + pyridine)$^+$, 304.2278; $C_{19}H_{30}NO_2$ requires 304.2276]; ν_{max}(paraffin mull)/cm^{-1} 3330s, 1120w, 1100s, 1070w, 1020m, 1005m, 905s and 870m; $\delta_H(CD_3OD)$ 1.53 (6 H, s), 1.63–1.89 (8 H, m), 2.0–2.2 (4 H, m), 2.29 (2 H, t) and 2.43 (2 H, m); m/z 224 (M^+, 1%), 206 (11), 191 (17), 188 (13), 173 (7), 163 (22), 135 (15), 121 (16), 107 (21), 105 (21), 95 (23), 93 (37), 91 (25), 81 (36), 79 (22), 71 (27), 67 (22), 55 (18), 45 (21), 43 (100), 41 (24) and 40 (21). The diol **8** was insufficiently soluble in common solvents for a ^{13}C NMR spectrum to be recorded. It is also very susceptible to elimination of water particularly in the presence of traces of acid.

Crystallography.—An Enraf–Nonius CAD4 X-ray diffractometer was used for all diffraction data collection. Details of the crystals used, the lattice dimensions and space groups, the diffractometry conditions and the collections of intensity data are presented in Table 1. The procedures used for the collection and reduction of intensity data have been described previously.[27] Weights, $w = 1/\sigma^2(F_o)$, were assigned to individual reflections with $\sigma(F_o)$ being derived from $\sigma(I_o) = [\sigma^2(I_o) + (0.04\ I_o)^2]^{\frac{1}{2}}$. All four structures were solved using a combination of direct methods (MULTAN)[28] and Fourier techniques. Details of the refinement of each structure follow.

Refinement of **5**. Refinement using standard procedures (BLOCKLS)[29] converged with $R = 0.17$. Refinement was continued using program RAELS[30] and incorporating 4 twin components (*hkl* which refined as a 36.6% component; $-hk\ -l$, 8.9%; $hk\ -\ l$, 31.4%; $-hkl$, 23.1%). The positions of all atoms were refined (except the z coordinate of the S atom) along with anisotropic thermal parameters. The hydroxy hydrogen atoms were included in positions determined from a difference map, and their positions were refined. All other hydrogen atoms were included in calculated positions. Each hydrogen atom was assigned an isotropic temperature factor

equivalent to that of the atom to which it was bound. Anomalous scattering[31] was included for all non-hydrogen atoms. The final residual was 0.023, and was not significantly different that that of the other enantiomer in space group $P4_3$.

Refinement of **6**. The structure was refined using BLOCK-LS[29] in the normal fashion. Hydroxy hydrogen atoms were included in map positions and were refined. All other hydrogen atoms were included in the refinement in calculated positions. Their temperature factors were maintained equal to those of the atoms to which they were bonded. Anomalous scattering[31] was included for all but the hydrogen atoms. Refinement converged with $R = 0.031$. When the other enantiomer was tested in space group $P4_3$, R fell to 0.030 and this was therefore adopted.

The structures of **5** and **6** are similar and related by the following transformations of coordinates: $x \leftrightarrow y$, $y \leftrightarrow x$, $z \leftrightarrow z$ and atom labels: S ↔ C(5'), C(1) ↔ C(5), and C(2) ↔ C(4).

Refinement of **7**. Conventional refinement using BLOCK-LS[29] converged with $R = 0.11$. Disorder of the molecule was evident in the difference map and was introduced. The molecule has an approximate two-fold axis nearly coincident with C(5)•••C(5') which, in this structure is aligned nearly parallel to *a* at (1/2, 1/2). In structure **7**, this pseudo two-fold axis is roughly perpendicular to the page. The second disorder component was obtained by rotating the molecule about this two-fold axis. In molecular terms, this involved placing the ethano bridge C(7)–C(7') where the methano bridge C(1) had originally been. The intensity data also showed pseudo-symmetry, leading to the pseudo space group *Pnan*. Refinement was continued (in $Pna2_1$) using a constrained refinement program (RAELS).[30] The second disorder component was treated as a rigid group identical with the original molecule, but its location and orientation were varied. When it became clear that the positions of the two oxygen atoms in the major and minor components had remained virtually the same, they were held at the same positions. This meant that the hydrogen bonding in the structure was unaltered by the existence of the disorder. Individual atoms of the major component were refined anisotropically (except that the thermal parameters of the two atoms of the ethano bridge were kept equal). Slack constraints were initially used to ensure that the geometry of the molecule remained reasonable, but these were all but removed in the final cycles. Thermal parameters of each atom of the minor component were fixed equal to those of the atom nearest to it in the major component. Hydroxy hydrogen atoms were included in the refinement in map positions, while all other hydrogen atoms were included in calculated positions. Hydrogen atom positions were not refined, their thermal parameters were kept equal to those of the atom to which they were bound. The occupancies of the two components refined to 73.7(8) and 26.3%. Anomalous scattering[31] was incorporated for O and C. Refinement converged with $R = 0.046$.

Refinement of **8**. Full matrix least squares was used for the refinement.[29] The hydroxy hydrogen atom was included in a position determined from a difference map and its position was refined. All other hydrogen atoms were included in calculated positions, allowing for the disorder of C(8) of the propano bridge, and were not refined. The temperature factors of the hydrogen atoms were maintained at the isotropic equivalent of those of the atoms to which they were bonded. All non-hydrogen atoms were refined with anisotropic thermal parameters. Anomalous scattering[31] was incorporated for the C and O atoms. An extinction correction was included. The final residual was 0.030.

Lists of positional parameters, thermal parameters, and structure factors for structures **5–8** have been deposited at the Cambridge Crystallographic Data Centre (CCDC).*

Acknowledgements

We thank Mrs. H. Stender for recording the NMR data, Dr. J. Brophy for obtaining the low resolution mass spectra and Mr. D. Nelson for determining the exact mass figures. Financial support by the Australian Research Council is gratefully acknowledged.

References

1 I. G. Dance, R. Bishop, S. C. Hawkins, T. Lipari, M. L. Scudder and D. C. Craig, *J. Chem. Soc., Perkin Trans. 2*, 1986, 1299.
2 I. G. Dance, R. Bishop and M. L. Scudder, *J. Chem. Soc., Perkin Trans. 2*, 1986, 1309.
3 E. Weber and H.-P. Josel, *J. Incl. Phenom.*, 1983, **1**, 79.
4 R. Bishop and I. G. Dance, in *Inclusion Compounds*, eds. J. L. Atwood, J. E. D. Davies and D. D. MacNicol, Oxford University Press, Oxford, 1991, vol. 4, pp. 1–26.
5 S. C. Hawkins, M. L. Scudder, D. C. Craig, A. D. Rae, R. B. Abdul Raof, R. Bishop and I. G. Dance, *J. Chem. Soc., Perkin Trans 2*, 1990, 855.
6 H. C. Brown and P. J. Geohegan, *J. Org. Chem.*, 1970, **35**, 1844.
7 R. Bishop, I. G. Dance and M. L. Scudder, *J. Chem. Soc., Chem. Commun.*, 1983, 889.
8 S. C. Hawkins, R. Bishop, I. G. Dance, T. Lipari, D. C. Craig and M. L. Scudder, *J. Chem. Soc., Perkin Trans. 2*, in the press, paper 3/02319B.
9 R. Bishop, S. Choudhury and I. Dance, *J. Chem. Soc., Perkin Trans 2*, 1982, 1159.
10 A. T. Ung, R. Bishop, D. C. Craig, I. G. Dance, A. D. Rae and M. L. Scudder, *J. Incl. Phenom.*, in the press.
11 P. C. Bulman-Page, D. J. Chadwick, M. B. van Niel and D. Westwood, *Acta Crystallogr., Sect. C*, 1987, **43**, 803.
12 M. M. Olmstead, W. K. Musker and B. D. Hammock, *Acta Crystallogr., Sect. C*, 1987, **43**, 1726.
13 A. Le Rouzic, D. Raphalen, D. Papillon and M. Kerfanto, *Tetrahedron Lett.*, 1985, **26**, 1853.
14 A. Le Rouzic, H. Patin and P. L'Haridon, *J. Chem. Res.*, 1988, (*S*) 288, (*M*) 2336.
15 T. B. Grindley, S. Kusuma and T. S. Cameron, *Can. J. Chem.*, 1986, **64**, 2388.
16 J. Golik, J. Clardy, G. Dubay, G. Groenewold, H. Kawaguchi, M. Konishi, B. Krishnan, H. Ohkuma, K. Saitoh and T. W. Doyle, *J. Am. Chem. Soc.*, 1987, **109**, 3461.
17 D. G. Brenner, *J. Org. Chem.*, 1985, **50**, 18.
18 R. M. Silverstein, G. C. Bassler and T. C. Morrill, *Spectrometric Identification of Organic Compounds*, Wiley, New York, 1981, 4th edn., pp. 195–196.
19 R. Bishop, I. G. Dance, S. C. Hawkins and M. L. Scudder, *J. Incl. Phenom.*, 1987, **5**, 229.
20 G. R. Desiraju, *Crystal Engineering: The Design of Organic Solids*, Elsevier, Amsterdam, 1989.
21 K. C. Pich, R. Bishop, D. C. Craig, I. G. Dance and M. L. Scudder, *Struct. Chem.*, 1993, **4**, 41.
22 R. Bishop, D. C. Craig, I. G. Dance, S. Kim, M. A. I. Mallick, K. C. Pich and M. L. Scudder, *Supramol. Chem.*, 1993, **1**, 171.
23 R. Bishop, D. C. Craig, I. G. Dance, M. L. Scudder, A. P. Marchand and Y. Wang, *J. Chem. Soc.. Perkin Trans. 2*, 1993, 937.
24 H. Stetter, H. Held and A. Schulte-Oestrich, *Chem. Ber.*, 1962, **95**, 1687.
25 B. R. Vogt, *Tetrahedron Lett.*, 1968, 1579.
26 R. Greenwald, M. Chaykovsky and E. J. Corey, *J. Org. Chem.*, 1963, **28**, 1128.
27 R. M. Herath Banda, I. G. Dance, T. D. Bailey, D. C. Craig and M. L. Scudder, *Inorg. Chem.*, 1989, **28**, 1862.
28 P. Main, S. J. Fiske, S. E. Hull, L. Lessinger, G. Germain, J.-P. Declercq and M. M. Woolfson, MULTAN80, A System of Computer Programs for the Automatic Solution of Crystal

* For details, see 'Instructions for Authors', *J. Chem. Soc., Perkin Trans. 2*, 1993, issue 1.

Structures from X-ray Diffraction Data, Universities of York and Louvain, 1980.
29 W. R. Busing, K. O. Martin and H. A. Levy, ORFLS, Report ORNL-TM-305, Oak Ridge National Laboratory, Tennessee, USA, 1962; BLOCKLS is a local version of this program.
30 A. D. Rae, RAELS, A Comprehensive Constrained Least Squares Refinement Program, University of New South Wales, 1989.
31 *International Tables for X-ray Crystallography*, Kynoch Press, Birmingham, vol. IV, 1974.

Paper 3/03691J
Received 28*th June* 1993
Accepted 15*th July* 1993